A Pressure Controlled Pinched Flow Fractionation Device for Continuous Particle Separation

T. L. Christiansen*[1], J. Trosborg*[1], S. Tanzi[1], S. T. Larsen[1], and R. Taboryski[1]

* These authors contributed equally to this research.
[1] Technical University of Denmark, Anker Engelundsvej 1, 2800 Kgs. Lyngby, Denmark

ABSTRACT

In this work the problem of separating small particles of different sizes is solved by developing a simple microfluidic device using pinched flow fractionation (PFF), a technique originally presented by Yamada et al. in 2004 [1]. The present work takes the concept of PFF to the next level by making the device tunable using a simple pressure control. Through analytical calculations and FEM simulations in COMSOL, the required dimensions and operating pressures of the device was determined. The device was subsequently fabricated by injection molding of a COC TOPAS grade 5013 polymer (TOPAS Advanced Polymers GmbH) using a micro machined silicon master. The functionality of the device was confirmed using polymer beads, and by adjusting the pressure accordingly a complete separation of 2 μm and 4.5 μm beads was demonstrated.

Keywords: pinched flow fractionation, pressure control, modified liga process, injection molding, cleanroom processing, microfluidics, point-of-care

1 INTRODUCTION

The recent advances in microfabrication technology has offered numerous novel ways of performing sample handling and analysis using cheap and compact devices, such as polymer lab-on-a-chips. Amongst these is the PFF device, in which no external fields are required as the particles are separated using only the properties of the laminar flow in the device. The fluids enter the PFF device from two separate inlets, one containing particles in a buffer solution and the other containing only buffer. The liquids then meet in a more narrow channel called the pinching segment, in which the particles are pushed up against one sidewall due to the pressure from the buffer liquid. The smaller particles will be very close to the wall, but due to their sizes, the center of the larger particles will be further from the wall. As the flow is laminar the particles will follow different streamlines, and the path of the respective particles can be regulated by controlling the direction of these flow lines, hence separating particles of different sizes by letting the flow lines terminate in different channels.

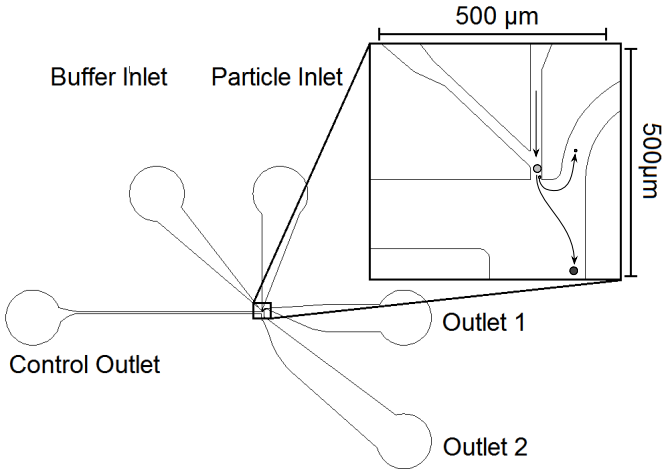

Figure 1: Illustration of the tunable pump controlled PFF device. The inset shows a detail of the pinching section. Small particles exits through outlet 1 while larger particles exits through outlet 2. The threshold size is determined by the pressure in the control outlet.

In this work, particles are separated in such a way that particles below a certain diameter threshold exits through outlet 1 while particles above this threshold exits through outlet 2, see Fig. 1. As opposed to existing PFF devices, the threshold can be continuously regulated by adjusting the pressure in the control outlet using a simple pump without use of on-chip valves [2].

2 DEVICE DESIGN

As seen in Fig. 1, the device consists of two inlets, a pinching segment and three outlets, of which one is solely used for regulating the size threshold via pressure control. The channel height is 22 μm as is the width of the pinching segment. This width was chosen based on previous work on PFF [1]. To estimate the diameter threshold, it is assumed that the total flow rate through the pinching segment, $Q_{p,tot}$, see Fig. 2, and the flow rates through the two outlets, Q_{T_L} and Q_{T_H}, are known. For steady-state flows, no generality is lost by setting $Q_{T_H} = \alpha Q_{T_L}$, where α is a proportionality constant dependent on the hydraulic resistances of the two outlet channels. Finally, the flow rate through the drain is set to $Q_{drain} = \mathcal{P} Q_{T_L}$, where $\mathcal{P}$ is a variable expressing the

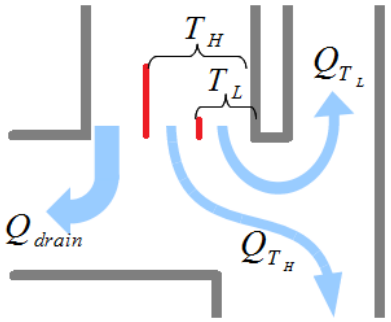

Figure 2: The concept of the device. All particles below a low threshold radius T_L go into outlet 1 and particles above T_L but below a high threshold radius T_H go into outlet 2 . All (unwanted) particles with radii above T_H will exit through the control outlet together with most of the buffer solution.

flow rate control due to the pump. The threshold value can be evaluated by assuming a parabolic velocity profile given by $v_x(y) = \frac{\Delta p}{2\eta L}(w_p - y)y$, where L is the length of the channel, w_p is the width of the pinching segment, η is the dynamic viscosity of the fluid and Δp is the pressure drop [3]. By furthermore using conservation of mass the equation describing the threshold diameter as a function of the variable $\mathcal{P}$ is given by

$$\begin{aligned} Q_{tot} &= (1+\alpha+\mathcal{P})Q_{T_L} \Leftrightarrow \\ \int_0^{w_p} dy v_x(y) &= (1+\alpha+\mathcal{P})\int_0^{T_L} dy v_x(y)\ . \end{aligned}$$

Solving this yields a relation between the threshold diameter and the flow parameter $\mathcal{P}$:

$$T_L^2(3w_p - 2T_L) = \frac{w_p}{(1+\alpha+\mathcal{P})}\ . \qquad (1)$$

By performing FEM simulations of the device in COMSOL, the optimal design of the channels can be found. The result of such simulations is seen in Fig. 3, where the flow lines of pinched particles having diameters of 1-10 μm is seen to be separated with a diameter threshold between 4 μm and 5 μm. The pressures used to achieve this is 0 mbar in outlet 1 and 2, 1 mbar in the particle inlet, 10 mbar in the buffer inlet and -20 mbar in the control outlet, which can be achieved using standard commercially available pumping equipment. The FEM simulations have also been used to find the relation between the flow parameter $\mathcal{P}$ and the pressure in the control outlet. Using this relation, Eq. (1) can be used to express the theoretical threshold diameter as a function of the pressure in the control outlet, which is plotted in Fig. 4.

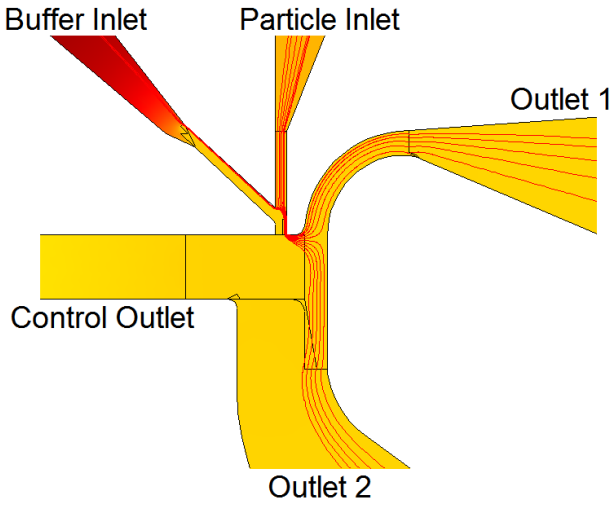

Figure 3: The figure shows a COMSOL simulation of the device at an under pressure of -20 mbar in the control outlet and a pressure of 1 mbar in the particle inlet and 10 mbar in the buffer inlet. Note that the figure only shows a part of the simulation; in fact, the entire device was simulated. The red lines are flow lines of pinched particles of diameter 1-10 μm with one μm interval and the colors indicate the pressure, yellow being low pressure and red being high pressure.

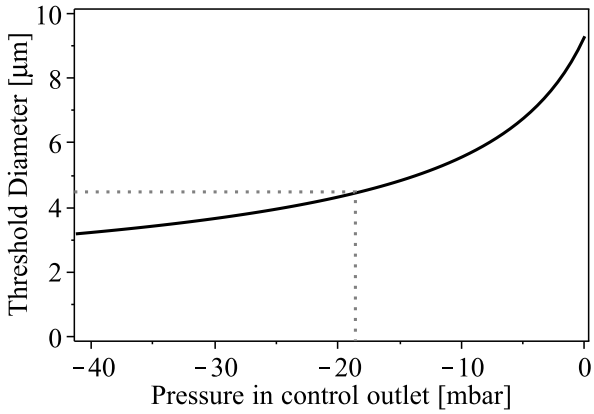

Figure 4: A plot of the analytical expression giving the threshold diameter as a function of the pressure in the control outlet. The dotted line indicates the pressure needed to set the size threshold at 4.5 μm, as this was the size relevant for the experiments in this work.

3 DEVICE FABRICATION

In the field of Lab-on-a-Chip systems, it is common practice to fabricate microfluidic devices in polymer which can offer cheap production costs, bio-compatibility and transparency. A well-known way of fabricating such devices is the LIGA process, where lithographically defined structures are electroplated to produce a negative of the structure in nickel, which can then be used as a mold for mass producing multiple replicas of the original structure in polymer [4]. In this work, a modified LIGA process is used, where the original structure is micro machined in silicon to achieve low roughness of the surface ensuring optimal bonding conditions. The result of this modified LIGA process is a nickel shim, which is inserted into an injection molder to fabricate the final polymer chip, see Fig. 5. In order to facilitate mass production of the devices, the polymer devices in this work are realized by the use of industrial scale injection molding equipment (Engel Victory 80/45 Tech). These polymer chips are then bonded to flat polymer disks, by pre-exposing the samples to 30" UV light from a mercury lamp (DYMAX mercury UV-bulb F/5000) followed by 5' thermal bonding at 120 °C and 10 kN in a conventional press (P/O/Weber).

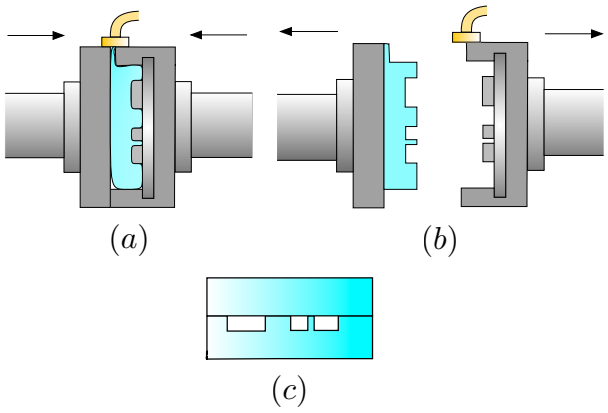

Figure 5: The figures illustrate the principle of the injection molding process. A polymer is heated up and injected into the mold where the shim is placed as seen in figure (a). Pressure is applied and after successful cooling of the mold and polymer, the mold is pulled apart, exposing the solid polymer disk, see figure (b). By bonding this polymer disk to a flat polymer disk, the microchannels are formed as shown in figure (c).

4 MEASUREMENTS & RESULTS

The measurements on the fabricated devices were performed using a setup with a LabView-controlled Festo 8 channel pressure regulator multi-channel pump capable of supplying both over- and underpressure as well as a Zeiss (Observer A1) microscope connected to a Zeiss

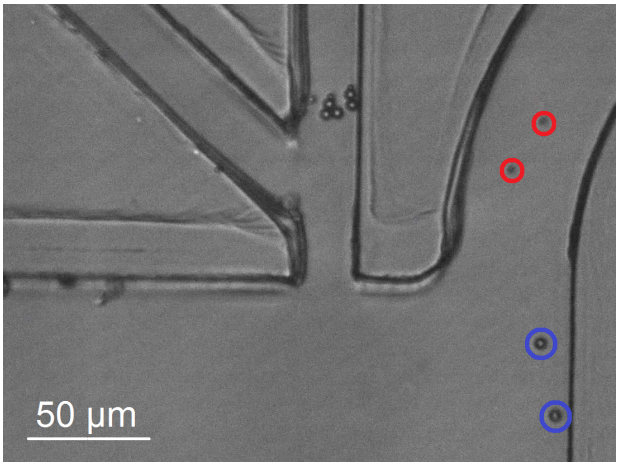

Figure 6: The micrograph shows how at a certain pressure threshold the particles will be separated in two different outlets. Beads of diameter 4.5 μm goes through outlet 2 and beads of diameter 2 μm goes through outlet 1. This measurement was performed at -17 mbar in the control outlet.

Axiocam Cml camera, enabling live recording of the experiments. Tubes were applied to all five ports of the device (two inlets and three outlets) such that the flow through the device could be completely controlled. A buffer solution was added to the buffer inlet, while the same solution containing polymer beads of diameter 2 μm and 4.5 μm, respectively, was added to the particle inlet. In principle, any bead diameter smaller than the size of the channel could have been chosen due to the tunability of the device, but the before mentioned sizes were chosen simply due to their distinguishability in the optical microscope.

By using the results from the FEM simulations in COMSOL, the pressure in the buffer channel inlet was set to 8 mbar while the pressure in the particle channel inlet was set to 2 mbar. Higher pressures could also have been used as only the ratio is significant, but the relatively low pressures were chosen in order to limit the particle speed and hence facilitate counting. Afterwards, the pressure in the buffer outlet was varied to see if the size threshold could be changed. For each pressure in the buffer outlet a movie of 30 second duration was recorded. This way about 100-200 particles would pass through the pinching segment, thereby giving a reasonable statistical basis for data treatment. After recording the movies, the number of 4.5 μm particles and 2 μm particles passing through outlet 1 and outlet 2 , respectively, was counted.

The pressure in the control channel was varied from -12 mbar to -21 mbar, as the theory predicts that the size threshold at -18 mbar is approximately 4.5 μm, see Fig. 4; hence, it should be possible to separate the two particle sizes at or slightly below this pressure. As seen

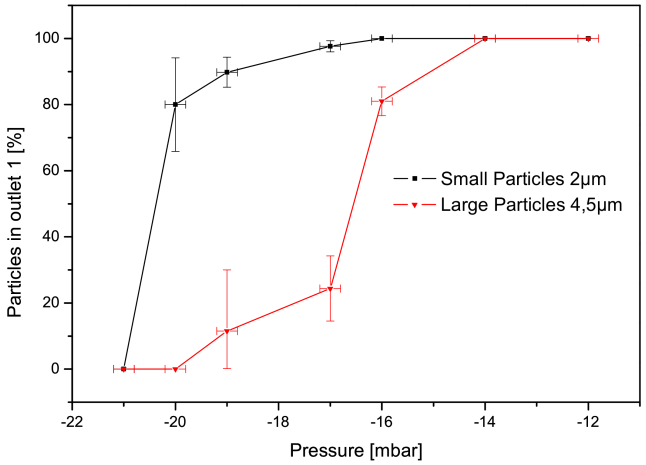

Figure 7: The figure shows the effect of changing the pressure in the control outlet while keeping the pressures in the other channels of the device constant. The percentage denotes the fraction of beads that pass through outlet 1. Each point corresponds to a 30 second run where 100-200 particles have been counted.

from the micrograph in Fig. 6, which was performed at -17 mbar in the control channel, the two different particle sizes are indeed separated as expected. This is also seen in the graph in Fig. 7, where each point corresponds to a 30 second run where 100-200 particles have been counted. Note that at low pressures in the control outlet numerically below -14 mbar all beads regardless of size flow through outlet 1 and if the pressure is numerically increased above -20 mbar, none of the beads will flow through outlet 1, as expected.

The transition from having all beads in outlet 1 to having none is somewhat indistinct, which can be contributed to the precision of the pump, leading to the pressure error bars in Fig. 7. This error could have been reduced by increasing the pressures while keeping the ratio. However, this would result in particle speeds which would inhibit counting of the beads. The vertical error bars originates from taking the standard deviation of the counted beads given by $\sigma_{\text{norm}} = \sigma_b/\sqrt{n}$. As the trajectory of each bead is indepedent from the trajectory of the other beads, it is reasonable to assume a binomial distribution, which has the standard deviation $\sigma_b = \sqrt{np(1-p)}$, where n is the total number of beads in a measurement and p is the fraction of beads that pass through outlet 1 [5]. As the number of particles per 30 second measurement is quite large, the fraction p can be estimated by using the measurements.

5 CONCLUSION

In this work it was shown that by adding a control channel to a standard PFF device, the particle size distribution in the outlet channels can be continuously tuned by the use of standard pumping equipment. As an example, it was demonstrated that polymer beads of diameter 2 μm and 4.5 μm, respectively, could be completely separated. This makes it possible to use a single chip design for multiple applications, while keeping the design as simple as possible, easing the fabrication. The simplicity of the design enabled mass production through a modified LIGA process using silicon micro machining and industrial injection molding equipment. Further work would include testing the device with biological materials such as cells for applications in life sciences.

6 ACKNOWLEDGEMENTS

This work is supported by the Danish Council for Strategic Research through the Strategic Research Center PolyNano (grant no. 10-092322/DSF).

REFERENCES

[1] M. Yamada, M. Nakashima and M. Seki, "Pinched Flow Fractionation: Continuous Size Separation of Particles Utilizing a Laminar Flow Profile in a Pinched Microchannel", Anal. Chem. 76, pp. 5465–5471, 2004

[2] Y. Sai, M. Yamada, M. Yasuda and M. Seki, "Continuous separation of particles using a microfluidic device equipped with flow rate control valves", Journal of Chromatography A 1127, pp. 214–220, 2006

[3] H. Bruus, "Theoretical Microfluidics", Oxford University Press, 2008.

[4] E. W. Backer, W. Ehrfeld, D. Mnchmeyer, H. Betz, A. Heuberger, S. Pongratz, W. Glashauser, H. J. Michel, and R. Siemens, "Production of separation-nozzle systems for uranium enrichment by a combination of X-ray lithography and galvanoplastics", Naturwissenschaften 69, pp. 520–523, 1982.

[5] R. A. Johnson, "Probability and Statistics for Engineers", Miller and Freund's, Seventh edition, 2005.